PLOS One

RESEARCH ARTICLE

# Characterization of the genomic landscape of canine oral osteosarcoma reveals similarities with appendicular osteosarcoma

**Christopher Husted[1,2☯], Sarah Adrianowycz[3☯], Cornelia Peterson[3], Suzanne Bartholf DeWitt[4], Elinor K. Karlsson[1,2], William Eward[5], Jason A. Somarelli[4], Kate Megquier[2‡*], Heather L. Gardner[3‡*]**

**1** UMass Chan Medical School, Worcester, Massachusetts, United States of America, **2** Broad Institute of MIT and Harvard, Cambridge, Massachusetts, United States of America, **3** Tufts University Cummings School of Veterinary Medicine, North Grafton, Massachusetts, United States of America, **4** Department of Medicine, Duke University Medical Center, Durham, North Carolina, United States of America, **5** Department of Orthopaedic Surgery, Duke University Medical Center, Durham, North Carolina, United States of America

☯ These authors contributed equally to this work.
‡ KM and HLG also contributed equally to this work.
* heather.gardner@tufts.edu (HLG), kmegq@broadinstitute.org (KM)

Check for updates

OPEN ACCESS

**Citation:** Husted C, Adrianowycz S, Peterson C, DeWitt SB, Karlsson EK, Eward W, et al. (2025) Characterization of the genomic landscape of canine oral osteosarcoma reveals similarities with appendicular osteosarcoma. PLoS One 20(6): e0325181. https://doi.org/10.1371/journal.pone.0325181

**Editor:** Filomena de Nigris, Universita degli Studi della Campania Luigi Vanvitelli, ITALY

**Received:** December 26, 2024

**Accepted:** May 8, 2025

**Published:** June 10, 2025

**Copyright:** © 2025 Husted et al. This is an open access article distributed under the terms of the Creative Commons Attribution License, which permits unrestricted use, distribution, and reproduction in any medium, provided the original author and source are credited.

**Data availability statement:** All whole genome sequencing data is available through the National Center for Biotechnology Information (NCBI) Sequence Read Archive (SRA) under BioProject PRJNA1154710.

## Abstract

Osteosarcoma (OS) is the most common bone tumor in both dogs and humans. It predominantly occurs in the appendicular skeleton, with about 25% of cases occurring within the axial skeleton. Progression of local disease is often the life-limiting factor for patients with axial OS, in contrast to appendicular OS, where local disease is addressed surgically, and metastatic disease remains the primary obstacle. While OS is a rare human cancer, limiting the availability of samples, its higher incidence in dogs provides a valuable comparative model for study. Both canines and humans share commonalities in clinical presentation, but dogs have an accelerated progression. Similarly, complex structural genetic changes define appendicular OS in both dogs and people, but it is unclear whether the genomic landscape of axial OS exhibits different alterations that may separate it from appendicular OS. We performed pilot whole genome sequencing of canine primary oral (maxillary or mandibular) OS tumors (n = 8) and matched normal tissue. We found that the genetics of canine oral OS largely parallel the genetics of canine appendicular OS, including an overall low number of recurrent point mutations affecting the same gene (*TP53* and *SETD2,* 3/8 samples). Structural variants dominated the landscape of mutational changes, with recurrent variants in *DMD* (4/8) and *DLG2* (3/8) found at a similar incidence to appendicular OS. This pilot suggests genomic similarities between oral and appendicular OS.

**Funding:** This publication was supported, in part, by the National Institutes of Health National Center for Advancing Translational Sciences under grant numbers UL1TR002733 and P30CA01658 (The OSU Biospecimens Repository), and the National Cancer Institute under grant numbers R01CA255319 and R37CA218570 (EKK). CP was supported by K01OD034451-01A1. KM was supported by a National Cancer Institute fellowship (F32CA247088). HLG was supported by K01OD028268-01A1. The content is solely the responsibility of the authors and does not necessarily represent the official views of the National Institutes of Health. The funders did not play any role in the study design, data collection and analysis, decision to publish, or preparation of the manuscript.

**Competing interests:** The authors have declared that no competing interests exist.

## Introduction

Osteosarcoma (OS) is the most common primary bone tumor in pediatric patients. While most patients develop OS in the appendicular skeleton, which includes bones of the limbs, primary tumors affecting the axial skeleton, including the spine, skull, and ribcage have also been reported. OS is uncommon and affects fewer than 1,000 people in the United States annually [1], and axial OS accounts for approximately 11% of this rare disease in people aged 0–24 [2]. Due to the proximity of axial tumors to critical structures, local tumor control and subsequent metastatic disease remain a pervasive clinical challenge. For people with unresectable axial tumors, 3-year survival rates are low, ranging from 11–56% [3]. Improved treatment options for patients with unresectable tumors or metastatic disease are needed, and a comprehensive knowledge of the tumor genome is important for enabling therapeutic development and precision medicine [4,5].

Canine OS is a valuable model system for osteosarcoma due to the approximately 10-fold higher disease incidence (estimated 13.9 compared to 1.02 per 100,000 dog or person-years at risk respectively), similar clinical presentation, and development of chemotherapy-resistant pulmonary metastatic disease [1,6]. Dogs also enable the evaluation of novel therapeutics in the setting of treatment-naive tumors and minimal residual disease [7]. As in people, appendicular OS is the most common form of OS in dogs, with approximately 12% of dogs developing the axial form of the disease [8]. The genomic landscape of canine appendicular OS is similar to the human disease, with copy number alterations in *MYC* and *DLG2* and a predominance of complex structural alterations [9]. Recent genomic characterization has clarified the unique advantages of this naturally occurring large animal model, underscoring its potential to bridge gaps between human patients and other model systems and enhance relevant human studies [1,7].

Oral OS, affecting the mandible or maxilla, is the most common form of axial OS [2,10,11]. It is unknown whether oral OS is genetically distinct from the more common appendicular OS. This information is critical to inform whether outcome-linked genetic characterization in appendicular OS is applicable to oral OS. The genomic landscape of human oral osteosarcoma remains largely unexplored, with whole-genome sequencing (WGS) data from only four samples of jaw or mandibular osteosarcoma published [12–14]. These limited datasets suggest that the genetic landscapes of oral and appendicular OS are similar; however, the small amount of available data precludes definitive conclusions.

There are no published WGS datasets of canine oral OS. Therefore, we conducted a pilot study of eight oral OS tumor-normal pairs with the main objectives of (1) exploring the genetic landscape of canine oral OS, and (2) performing a preliminary comparison of canine oral OS to canine appendicular OS.

## Materials and methods

### Sample acquisition and DNA extraction

Matched canine primary tumor and normal tissue samples were provided by The Ohio State University Biospecimen Repository (n = 7), and the Canine Comparative

Oncology Consortium (CCOGC) [15] (n = 1). Genomic DNA was isolated from flash-frozen tumors and normal tissue samples using the DNeasy Blood & Tissue Kit (Qiagen Inc., Hilden, Germany) per manufacturer instructions. Sample collection was approved by the Institutional Animal Care and Use Committees at the collecting institutions (The Ohio State University protocol number 2010A0015-R5, University of Wisconsin-Madison protocol number V005297).

### Histopathological assessment

Hematoxylin and eosin-stained (H&E) tissue sections were available for review by a single board-certified veterinary pathologist for 5 of the 8 samples to confirm the initial clinical diagnosis and histologic subtype and to estimate the percentage of tumor and necrosis in each sample. Tumor fraction was computationally estimated in all eight samples using the ichorCNA tool [16], as histologic slides were unavailable for review in 3 cases [16].

### Library construction and sequencing

Library preparation and whole genome sequencing (WGS) were performed by the Broad Institute Genomics Platform, as previously described [9]. Briefly, 100 nanograms of genomic DNA was prepared using the KAPA Hyper Prep Kit with Library Amplification Primer Mix (KAPA Biosystems; #KK8504) with palindromic forked adaptors containing a unique 8-base index sequence (Roche). Libraries (2.2nM each) were pooled and sequenced on an Illumina HiSeqX using 151 base pair paired-end reads. Normal tissue samples were sequenced to a target depth of 30x and tumors to a target depth of 60x. The mean sequencing depth achieved was 51x (range 43X - 57x) for normal samples and 95x (range 70x - 119x) for tumor samples.

### Preprocessing of sequencing data

Fastq files were aligned to the canine reference genome (CanFam4, UU_Cfam_GSD_1.0 [17] with the Y chromosome sequence from the ROS_Cfam_1.0 assembly appended [18,19]) using BWA, and were preprocessed following GATK best practices [17–23]. For all GATK tools, version 4.2.3.0 was used unless otherwise stated. Duplicate reads were identified using Picard Tools MarkDuplicates (http://broadinstitute.github.io/picard). Base Quality Score Recalibration (BQSR) was performed using a VCF file of germline variants from 1987 dog and other canid samples [18,23].

### Simple somatic mutation calling

Simple somatic mutations (single nucleotide variants (SNVs) and small insertions and deletions (indels)) were detected using a consensus calling approach combining three somatic mutation callers: Mutect2, Strelka2, and VarScan2 (**Fig 1**) [24–26]. Mutect2 was run with the germline reference file from 1987 dogs and other canids and a panel of normals of 40 dogs (including the eight reported in this study). Additional arguments "—downsampling-stride 20," "—max-reads-per-alignment-start 6," and "—max-suspicious-reads-per-alignment-start 6" were used in running Mutect2. FilterMutectCalls was run with the "—run_orientation_bias_mixture_model_filter" option set to "True" and the "—min-median-read-position" option set to 10 bp. A VCF file containing common (allele frequency between 0.01 and 0.2) germline variants was used in the CalculateContamination step. The default settings for tumor-normal calling were used for Strelka2 and VarScan2. The mutation calls from each tool that passed filtering were processed through bcftools [27] isec to obtain a consensus. Only mutation calls identified in two or more callers were retained for downstream analysis. The KaryoploteR package, using R (R4.4.0), was used to identify areas of kataegis [28]. Lollipop plots were created using the lollipops tool [29].

### Structural variant calling

Structural variants (SVs) were called using Manta version 1.6.0 in the tumor-normal configuration [30]. The output VCFs were processed using the Manta-provided script "convertInversion.py" to convert inversions to the older INV format rather than the break end (BND) format. The calls were then processed using bcftools, removing any calls where the "FILTER"

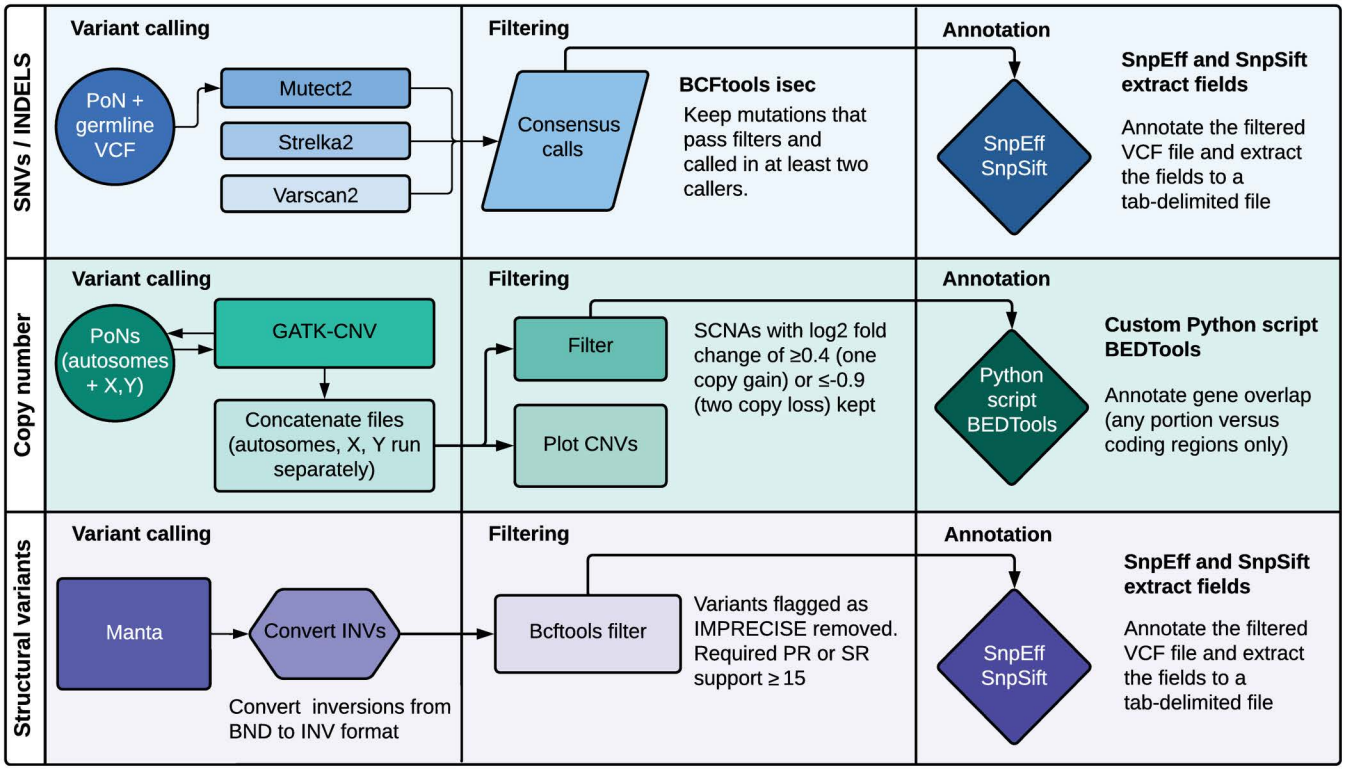



**Fig 1. Overview of somatic calling workflow.** Workflow showing the tools and settings used to call simple somatic variants, copy number variants, and other structural variants.

https://doi.org/10.1371/journal.pone.0325181.g001

flag was not set to "PASS", that were marked as imprecise (IMPRECISE = 1), or where neither the paired read (PR) or split read (SR) support was 15 reads or more.

### Somatic copy number aberration calling

Somatic copy number aberrations (SCNAs) were detected using the GATK somatic CNV pipeline in tumor-normal mode [20,21]. Four panels of normals were created using germline samples from dogs included in this study, plus 32 additional dogs with a cancer diagnosis—one containing the autosomes, male-only and female-only panels for chromosome X, and one male-only panel for chromosome Y. SCNAs were called on the autosomes and chromosomes X and Y separately, as recommended. Copy number losses with a log2 fold change of ≥0.4 (one copy gain) or ≤−0.9 (two copy loss) were considered for analysis.

### Oncoprint visualization

The filtered somatic mutations were plotted as an oncoprint using the PyOncoprint [25] Python package, with additional annotations added in Adobe Illustrator 2023. Genes were included in the oncoprint based on the following criteria: (1) genes with alterations in more than three samples; (2) genes with alterations in three samples and either commonly reported in the OS literature or found in the COSMIC Cancer Gene Census Tier 1 genes; (3) genes that were recurrently altered in our dataset and not previously reported in canine OS; and (4) genes that were recurrently altered in our dataset and linked to inherited osteosarcoma syndromes, bone cancer, or sarcoma in the COSMIC database [12,31,32].

Structural variants are displayed as "multi-hits" when more than two variant types are present within the same gene in a single sample. Simple somatic mutations are represented as "multi-effect" when a single mutation results in multiple effects in one or more gene transcripts.

### Coding exon overlap

To summarize somatic copy number aberrations and other structural variants which overlap coding regions of genes, we used the BEDTools [33] "annotate" function to count the number of mutations in each sample overlapping the CDS regions of the CanFam4 genome. These counts were then aggregated to the gene and sample levels.

### Mutational signature calling

The SigProfilerMatrixGenerator tool was used to generate a matrix of variant mutational contexts, and all samples were run through CrossMap (v0.7.0) to lift over the mutations from CanFam4 to Canfam3.1 [34,35]. We then used the SigFit tool (v2.2) to identify the COSMIC v3 single base substitution (SBS) signatures in the oral osteosarcoma data [12,36]. Fitting was run with 10000 iterations and 5000 warmup iterations using the multinomial model. Signatures sufficiently greater than zero (meaning that the lower end of the Bayesian HPD interval was > 0.025 in any sample) were selected, and fitting was rerun using only those signatures.

### Pathway analyses

Pathway analysis was performed using the STRING Database [37] app on the Cytoscape desktop tool, version 3.10.3 [38]. Species was set to *Canis lupus familiaris*, background was set to "whole genome", confidence score cutoff was set at 0.5, and maximum additional interactors were set at 0. Gene lists for individual pathways were downloaded from MSigDB [39,40], including "Chromatin Modifying Enzymes" and "Neurexins and neuroligins" from Reactome [41], "Cell Cycle" and "MAPK Signaling Pathway" from the Kyoto Encyclopedia of Genes and Genomes (KEGG) [42], and "Phosphatidylinositol 3 Kinase Protein Kinase B Signal Transduction" from the Gene Ontology Biological Processes [43,44]. Protein interactions were defined using the STRING Database and The Human Protein Atlas [45,46].

## Results

### Cohort characteristics

Patient demographics were consistent with published data [47,48]. The median age at diagnosis was 9 years (range 5–12 years). The most common breeds were Labrador retriever (n = 3) and mixed breed (n = 3). The other included breeds (n = 1 each) were boxer and bullmastiff. Five of eight (62.5%) dogs were female (four spayed, one intact), and three were castrated males. Two tumors were maxillary in origin, and six were mandibular in origin. Full patient demographic and clinical metadata is available in S1 Table.

### Histopathological assessment

H&E slides were available for 5 of the 8 samples for review by a pathologist to confirm the diagnosis of OS, histologic subtype, and estimate the percentage of tumor tissue and necrosis in each sample (Fig 2, S1 Fig). Four tumors were mandibular and one maxillary. Five OS subtypes were represented: chondroblastic, fibroblastic, mixed, osteoblastic, and poorly differentiated osteoblastic. The approximate percentage of the proportion of neoplastic cells ranged from 70–95%, with a median of 87%. The estimated percentage of tissue necrosis ranged widely from <10% to 40%, with a median of approximately 15%. Since H&E slides were not available for review in 3 dogs (Axial-OS-03, Axial-OS-07, Axial-OS-08), tumor content was also assessed computationally using the ichorCNA tool. The histologic and computational assessment of tumor content were highly correlated (Spearman's rho = 0.82, p-value: 0.09) (**Fig 2A**). The

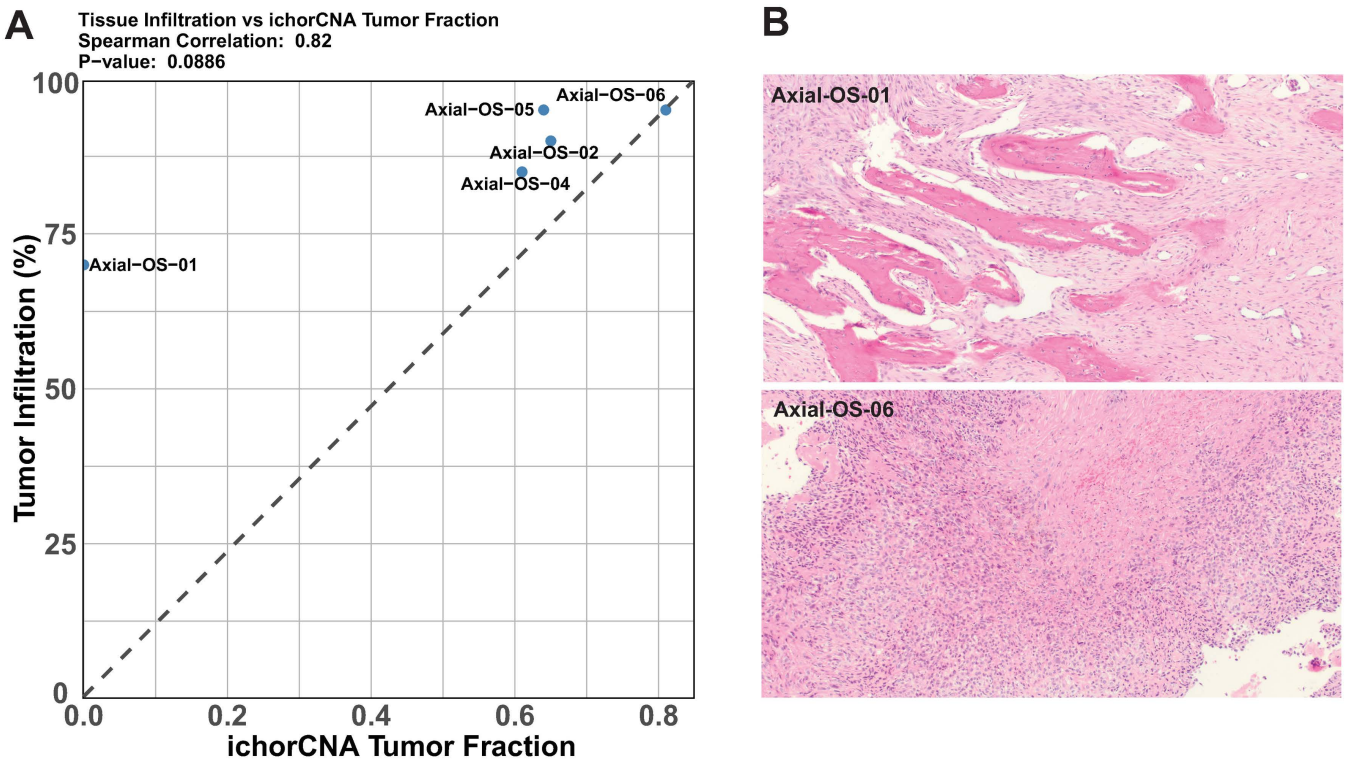



**Fig 2. Assessment of tumor content.** A. Correlation plot of the samples where we have both tumor fraction obtained from ichorCNA and percent neoplastic cells in the tumor mass as determined by a pathologist. B. Histological images of two canine oral osteosarcoma samples with the highest and lowest fraction of tumor infiltration.

https://doi.org/10.1371/journal.pone.0325181.g002

ichorCNA derived tumor fractions ranged from 0–81%, with a median of 64% (**Fig 2B**). One sample (Axial-OS-01) was an outlier, with the pathologist estimate of neoplastic cells of 70%, but an ichorCNA tumor fraction estimate of 0. The cause of this discrepancy is unknown, but possible contributing factors include sampling disparities between the frozen and fixed specimens in the context of tumor heterogeneity and low numbers of large-scale copy number changes in the tumor.

### Simple somatic mutations in canine oral OS

We identified recurrent mutations in key genes such as *TP53* (n = 3) and *SETD2* (n = 3). The median number of simple somatic mutations (SNVs or INDELs) per sample was 21 coding (range 1–72) and 2702 non-coding (range 188–9327). The non-coding and coding SNV counts per sample were highly correlated ($r = 0.95$, $p = 0.0002$). Missense mutations were the most common coding SNV identified (64%) (Fig 3). Consistent with findings in canine appendicular OS samples [9,49,50], *TP53* and *SETD2* were mutated in multiple samples (3/8; 38%) (Fig 4, S3 Table). In *TP53*, we observed several mutations across multiple dogs in the P53 DNA binding domain and one frameshift mutation in the P53 transactivation domain. *SETD2* mutations were not clustered in a particular domain or location (Fig 4). Five additional genes had recurrent coding mutations (2/8 samples each, 25%) — *DNAI2* and *SH3BGRL2*, which have been shown to be differentially expressed in human OS [51,52], and *CCDC60*, *FCRL5*, and *IMMP2L*, which have not previously been reported in OS.

Noncoding SNVs and INDELs (within untranslated regions (UTRs), introns, or upstream or downstream of the gene) were identified in several genes mutated in published human and dog OS datasets. Four genes had noncoding variants associated with them in all 8 samples, all of which have been previously described as altered in human or canine OS:

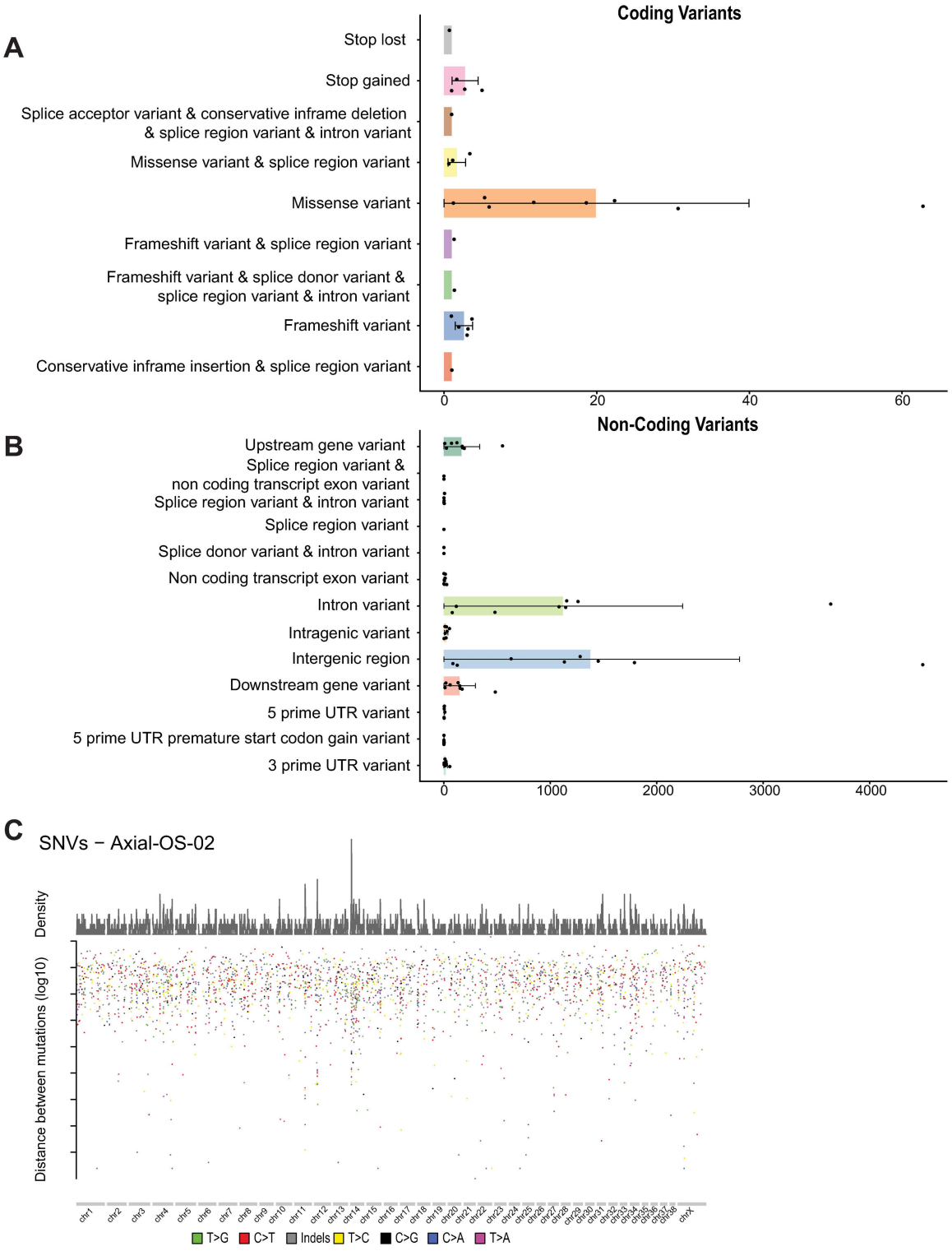



**Fig 3. A. Frequency of coding single nucleotide variants and B. non-coding single nucleotide variants; C. Rainfall plot showing focal hyper-mutation in Axial-OS-02.**

https://doi.org/10.1371/journal.pone.0325181.g003

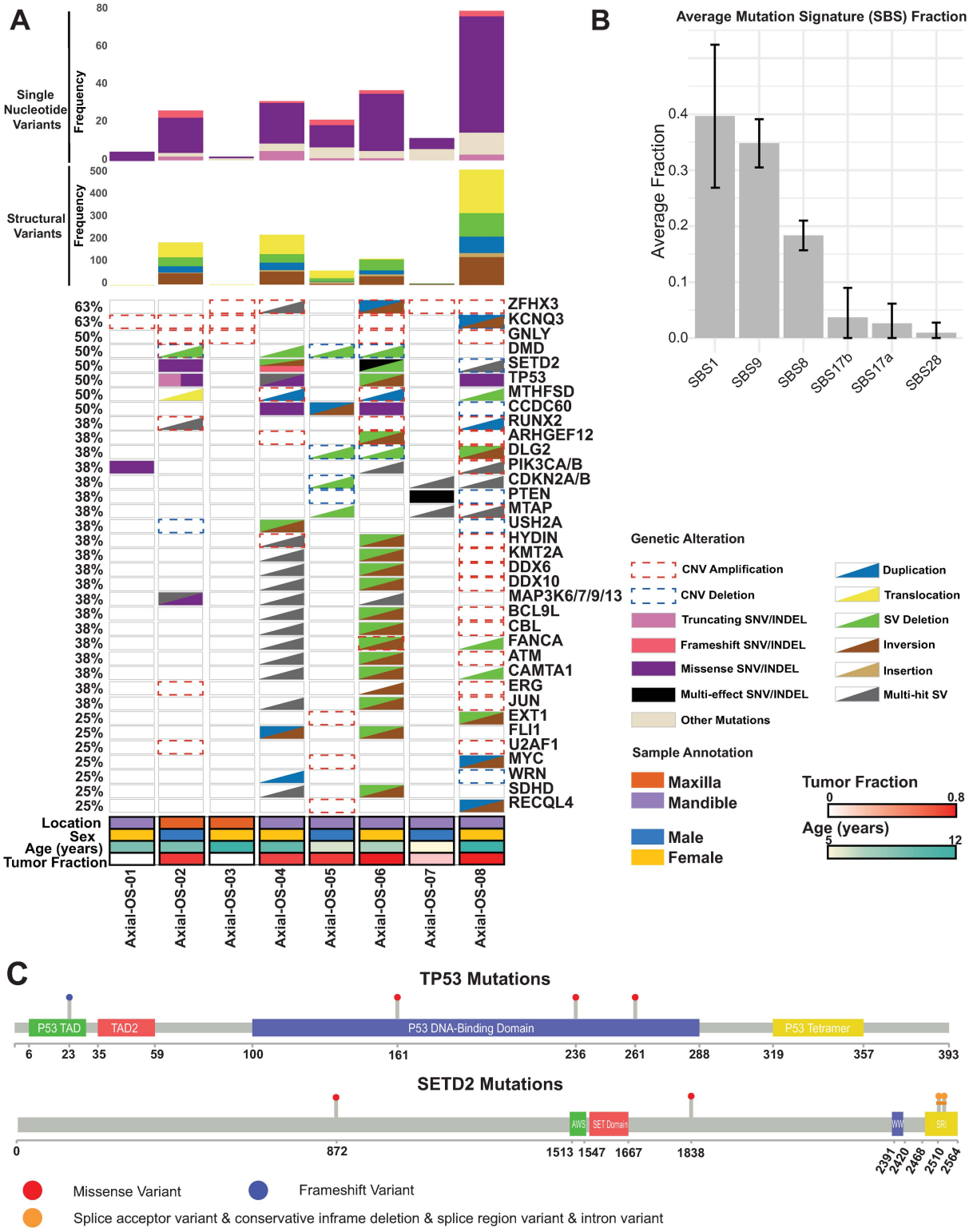



**Fig 4. A. Oncoprint represents the key simple somatic mutations, copy number aberrations, and other structural variants in recurrently altered or known osteosarcoma genes; B. Barplots summarize the most common single base substitution (SBS) signatures. Error bars represent the mean exposure ± standard deviation (SD); C. Lollipop plots showing mutations in TP53 and SETD2 proteins.**

https://doi.org/10.1371/journal.pone.0325181.g004

*DMD*, *DLG2* [9,53], *CCSER1* [54], and *NAALADL2* [55]. An additional nine genes were associated with noncoding mutations in 7/8 (88%) of samples, including *MAGI2*, *CTNND2,* and *CSMD1*, which have been reported to be altered in OS [53].

In canine appendicular OS, regions of focal hypermutations indicative of kataegis have been reported [9]. Using a modified maftools [56] "kataegis_detect_chr" function, we identified a single hypermutated region on chromosome 14 in the Axial-OS-02 sample (Fig 3). No distinct patterns of hypermutation were detected in the other samples (S2 Fig).

### Structural variants in canine oral OS

Structural variants (SVs) were identified, including translocations, inversions, insertions, deletions, and duplications (Fig 5, S4 –S6 Tables). The median incidence was 84 per sample (range 1–481). The most common SVs were inversions (n = 256) and deletions (n = 232). Insertions were less commonly identified (n = 41) and were predominantly noncoding, with only one affecting a coding region of the gene *PSKH1*.

Recurrent structural variants were found in the *MTHFSD* gene (n = 4 samples), as well as *CDKN2A*/*B*, *DMD*, *DLG2, MTAP*, and *SETD2* (n = 3 samples each). Deletions were most common, although inversions, duplications, and translocations were identified in addition to deletions in some samples. In addition, several cancer-associated genes on chromosome 5 tended to be altered together or in similar ways, including *CBL*, *BCL9L*, *DDX6*, *DDX10*, *ATM*, *JUN*, *SKI*, *CAMTA1*, *PIK3CD*, *FANCA*, and *HYDIN*.

### Somatic copy number aberrations in canine oral OS

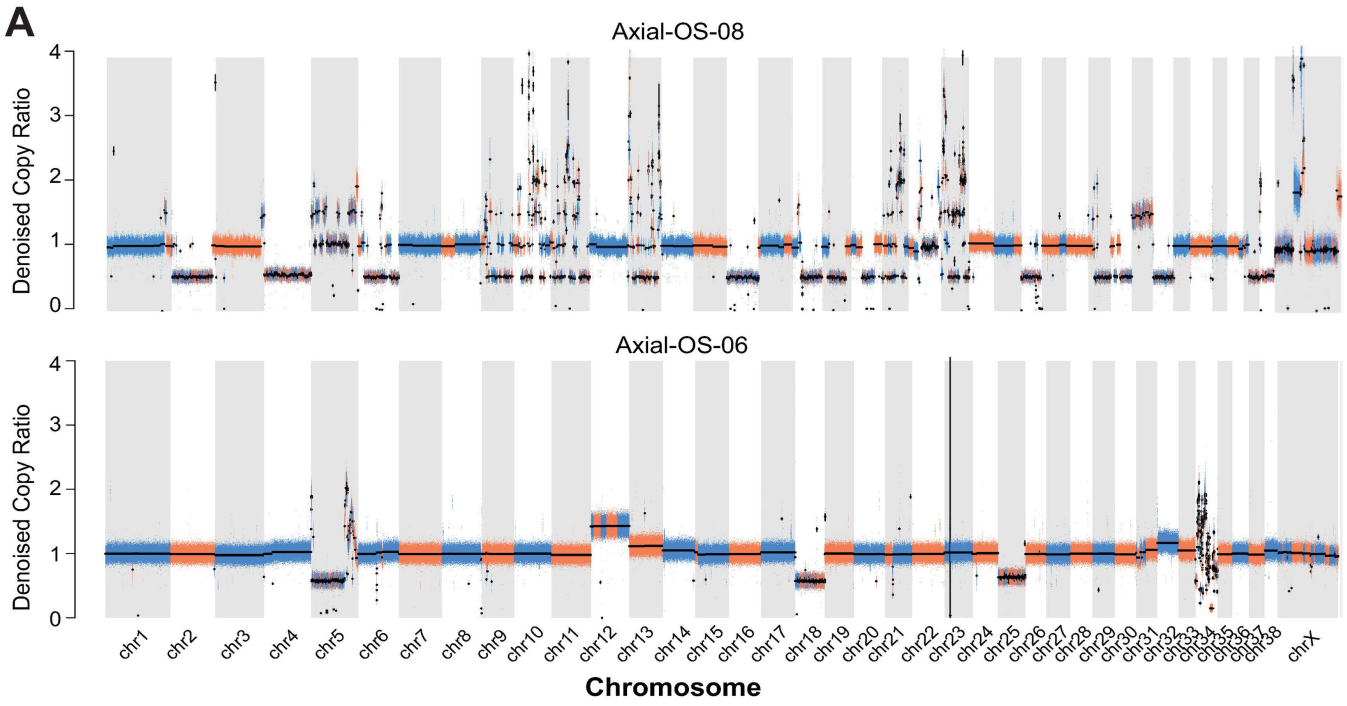
The most common copy number gains ($\log_2$ fold change ≥ 0.4) identified were in the tumor suppressor *ZFHX3* (5/8, 63%), the cytolytic granule protein gene *GNLY* (4/8, 50%), and the potassium voltage-gated channel gene *KCNQ3* (4/8, 50%) (S7 and S8 Tables, S3 Fig). Common copy number losses ($\log_2$ fold change ≤ −0.9) were seen s in *DLG2* (3/8, 38%), which has commonly been reported as deleted in OS [57]. Less common recurrent alterations included gains of the *RUNX2* oncogene and tumor suppressor *ARHGEF12* (3/8, 38%), and loss of *DMD* and the PI3K pathway tumor suppressor *PTEN* (2/8, 25%), all of which have been previously identified as altered in appendicular OS [9,53,57]. While copy number gains in *MYC* were present in fewer samples (1/8, 12%) than reported in canine appendicular OS (36%) [9], we lack statistical power to assess whether this is a true difference in affected driver genes or whether it is due to chance in a small cohort.

### Mutational signatures in canine oral OS

The trinucleotide context of SNVs was evaluated to identify mutational signatures defined by COSMIC v3. Signatures identified included: SBS1 (the "aging signature," associated with spontaneous deamination of 5-methyl-cytosine), SBS8 (unknown etiology), SBS9 (possibly due to somatic hypermutation via polymerase eta in lymphoid cells), SBS17a (unknown etiology), SBS17b (associated in some human cases with fluorouracil chemotherapy and reactive oxygen species damage), SBS28 (unknown etiology) (Fig 4, S4 Fig) [32]. SBS1 made the highest contribution, while the lowest was made by SBS28. Many of these signatures have been previously reported in human or canine OS, with the exception of SBS28 [9,49,50].

### Pathways analysis of canine oral OS samples

We performed pathway analysis of 2785 genes with any recurrent coding mutation (altered in two or more samples). Of these, 2259 genes mapped to identifiers in the STRING Database. These genes were most enriched in immune-related pathways such as the KEGG Cytokine-cytokine receptor interaction (FDR = 1.7E-3) and Hippo signaling (FDR = 6.6E-3) pathways (S9 Table). The 183 genes with a coding SNV/INDEL in any sample (as too few genes had recurrent mutations to allow pathway analysis) mapped to 154 identifiers. These coding SNVs/INDELs were enriched in pathways including



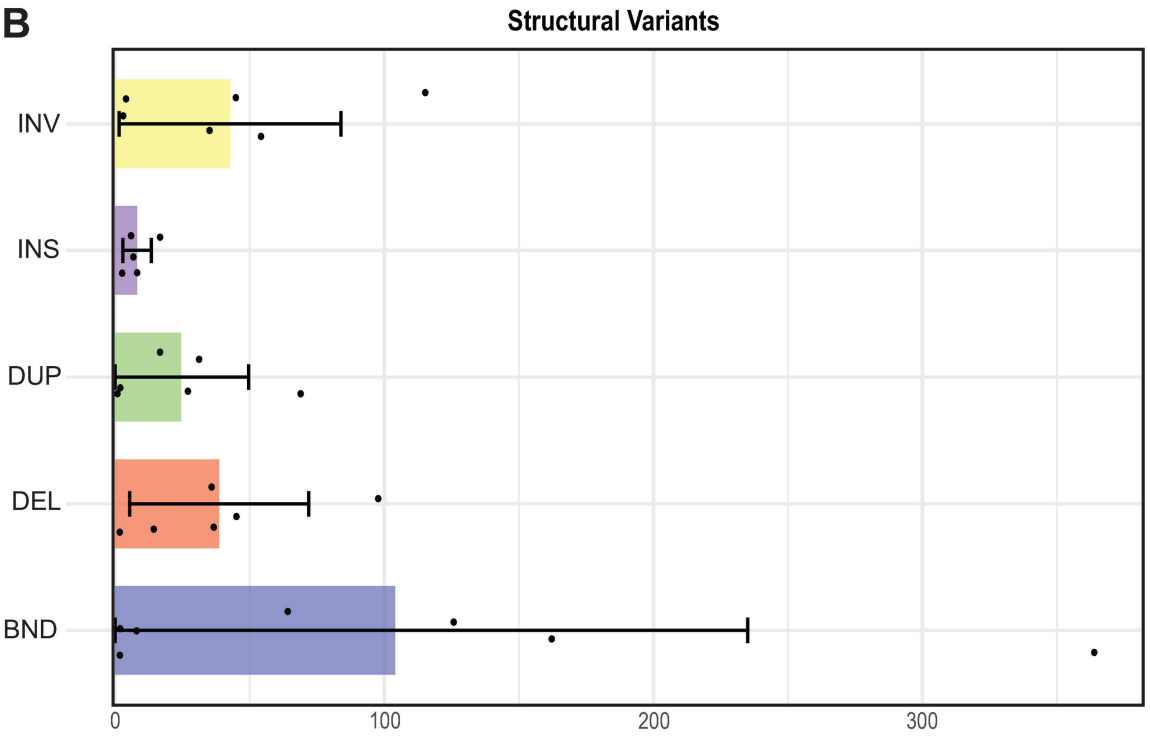




**Fig 5. A. Copy Number ratio plots illustrating the locations of both focal and whole-chromosome copy number aberrations in Axial-OS-08 and Axial-OS-06; B. Barplots of the frequency of Structural Variant types across canine oral osteosarcoma samples.** Error bars represent the mean exposure ± standard deviation (SD), with the lower bound adjusted to zero if below this value.

https://doi.org/10.1371/journal.pone.0325181.g005

KEGG Central Carbon Metabolism in Cancer (FDR = 0.0046) and PI3K-Akt Signaling (FDR = 0.029), and the GO molecular function Protein tyrosine phosphatase activity (FDR = 0.022) (S10 Table). In contrast, the 1479 genes with recurrent noncoding mutations (UTR, intron,1025 identifiers) were most enriched in the "Nervous System" tissue compartment (FDR = 1.42E-28) as well as pathways including the Reactome "Neuronal system" (FDR = 4.01E-16) (S11 Table). Investigating this enrichment further, we noted that 4/8 samples had 3'UTR mutations in genes in the "Neurexins and Neuroligins" pathway (*NRXN1*, *NRXN3*, *DLGAP2*, and *EPB41L3*). Overall, 7/8 of our samples had some kind of alteration in this pathway (S11 Table).

Previous studies of canine appendicular OS have highlighted common mutations in the PI3K and MAPK pathways and genes involved in cell cycle and chromatin remodeling [9,53]. We investigated how many genes in each pathway were mutated in oral osteosarcoma by the different mutation types (S12 Table). The PI3K/AKT pathway was most commonly altered, with 6/8 samples having simple somatic mutations, 6/8 samples having structural variants, and 5/8 samples having somatic copy number aberrations. Chromatin Modification and Epigenetic Pathways were also commonly affected, 4/8 samples by simple somatic mutations, 6/8 samples by structural variants, and 5/8 samples by somatic copy number aberrations.

## Discussion

We sought to explore the genomic landscape of canine OS to determine whether genetic features of OS were conserved between appendicular and oral tumors. Overall, we found similarities between oral OS and reported genomic features of appendicular OS in dogs. Structural variants predominate in both tumor locations. *SETD2* and *DMD* were mutated in half of our samples, recapitulating the features of appendicular canine OS [9]. The p53 and PI3K pathways were altered in 38% of samples, and genes involved in chromatin regulation were altered in 50% of samples, frequencies similar to those previously reported in appendicular OS [9].

We identified several genomic features in this cohort to prioritize for further exploration in larger cohorts. The most common copy number gains were in *ZFHX3* and *KCNQ3*. *ZFHX3* is a transcription factor and negative regulator of c-Myb [58] that has been previously reported as gained in canine OS [9,59], and has been shown to be altered in a mutually exclusive manner with *MYC* in human cancers [60]. *KCNQ3* encodes a potassium voltage-gated channel which has been shown to increase MYC and Wnt pathway activity in gastroesophageal adenocarcinomas [61]. All samples in our study had copy number gains in either *ZFHX3*, *KCNQ3*, or *MYC*, while two samples had concurrent alterations in *ZFHX3* and *KCNQ3*, suggesting that alterations in these genes may have a similar or complimentary functional role in oral OS tumors.

Another interesting feature of our dataset was the recurrent alteration of the neurexin and neuroligin pathway, which includes the *DLG2* gene commonly altered in appendicular OS. While genes in this pathway are mainly known for their role in synapses, they have also been shown to play an important role in the vascular system [62–64]. In cancer, they promote colorectal cancer progression through the APC/β-catenin pathway [65], are overexpressed in non-small-cell lung cancer [66], are associated with poor prognosis in Ewing's sarcoma [67], and have been reported to facilitate bone cancer pain [68]. Collectively, our findings highlight neurexins and neuroligins as candidates for further study in oral OS.

The primary limitation of this exploratory study is the small sample size. Larger studies will be essential to generate a more comprehensive understanding of genetic alterations in oral OS and to compare and contrast genomic alterations between appendicular and oral OS in dogs and humans. An additional limitation of this study was the low tumor fraction of some of our samples. In our study, two samples (Axial-OS-01 and Axial-OS-03) had ichorCNA-estimated tumor fractions below 10%, which likely hindered our ability to identify somatic alterations in these samples. Due to the small sample size and lack of comprehensive clinical metadata, we were also unable to explore the potential effects of tumor subtype, grade, and stage on the tumor genome.

## Conclusions

Our canine oral osteosarcoma dataset is defined by high structural complexity and few recurrent point mutations and demonstrates broad genetic concordance between oral and appendicular OS. We highlight copy number gains in *ZFHX3* and *KCNQ3* and alteration of the neurexin and neuroligin pathway for further exploration. Prospective studies with larger sample sizes will be necessary to further characterize the genetic landscape of oral OS.

## Supporting information

**S1 Table. Clinical metadata and tumor fraction.** Clinical metadata including breed, age, sex, tumor site, tumor size, ichorCNA tumor fraction, and treatment information.
(XLSX)

**S2 Table. Sequencing information.** Sequencing metrics from platform for each axial osteosarcoma sample.
(XLSX)

**S3 Table. Simple somatic mutations.** All simple somatic mutations that passed filters.
(XLSX)

**S4 Table. Structural variants.** Structural variants called by Manta that passed filters, annotated by Snpeff.
(XLSX)

**S5 Table. Chromosome-level structural variants.** Structural variants that are classified "chromosomal" and the genes within those regions in each sample.
(XLSX)

**S6 Table. Coding structural variants. A.** Translocations, **B.** Deletions, **C.** Duplications, **D.** Insertions, **E.** Inversions. Samples with no coding variants are omitted.
(XLSX)

**S7 Table. Somatic copy number aberrations.** Copy number variants and overlapping genes within the variant regions called in each axial osteosarcoma sample.
(XLSX)

**S8 Table. Coding somatic copy number aberrations.** Somatic copy number aberrations and overlapping genes filtered to variants that overlap exon regions of genes.
(XLSX)

**S9 Table. Pathway enrichment of all mutation types.** Results of STRING Database pathway enrichment for all genes with mutations in two or more samples.
(XLSX)

**S10 Table. Pathway enrichment of coding mutations.** Results of STRING Database pathway enrichment for all genes with coding mutations.
(XLSX)

**S11 Table. Pathway enrichment of noncoding simple somatic mutations.** Results of STRING Database pathway enrichment of mutations non-coding simple somatic mutations seen in two or more samples.
(XLSX)

**S12 Table. Somatic mutations in commonly altered pathways.** Somatic mutations in commonly altered pathways in OS.
(XLSX)

**S1 Fig. Tumor histology.** Images of hematoxylin and eosin-stained histology slides from samples **A.** Axial-OS-02, **B.** Axial-OS-04, and **C.** Axial-OS-05.
(PDF)

**S2 Fig. Rainfall plots.** Rainfall plots for every axial osteosarcoma sample with density plots with distance between mutations in $\log_{10}$ scales.
(PDF)

**S3 Fig. Copy number segmentation plots.** Denoised copy number segmentation plots with the copy number segments represented in blue and orange. Black line represents the denoised median.
(PDF)

**S4 Fig. Mutational signature plots.** Mutational signature composition of each sample.
(PDF)

## Author contributions

**Conceptualization:** William Eward, Jason A Somarelli, Kate Megquier, Heather L Gardner.

**Data curation:** Christopher Husted, Sarah Adrianowycz, Cornelia Peterson, Kate Megquier, Heather L Gardner.

**Formal analysis:** Christopher Husted, Sarah Adrianowycz, Kate Megquier, Heather L Gardner.

**Funding acquisition:** Elinor K Karlsson, William Eward, Jason A Somarelli, Kate Megquier, Heather L Gardner.

**Methodology:** Christopher Husted, Kate Megquier, Heather L Gardner.

**Resources:** Elinor K Karlsson, William Eward, Jason A Somarelli, Kate Megquier, Heather L Gardner.

**Supervision:** Elinor K Karlsson, Kate Megquier, Heather L Gardner.

**Visualization:** Christopher Husted, Kate Megquier, Heather L Gardner.

**Writing – original draft:** Christopher Husted, Sarah Adrianowycz.

**Writing – review & editing:** Christopher Husted, Sarah Adrianowycz, Cornelia Peterson, Suzanne Bartholf DeWitt, Elinor K Karlsson, William Eward, Jason A Somarelli, Kate Megquier, Heather L Gardner.

## References


1. Beck J, Ren L, Huang S, Berger E, Bardales K, Mannheimer J. Canine and murine models of osteosarcoma. Vet Pathol. 2022;59:399–414.
2. Mirabello L, Troisi RJ, Savage SA. Osteosarcoma incidence and survival rates from 1973 to 2004: data from the surveillance, epidemiology, and end results program. Cancer. 2009;115(7):1531–43. https://doi.org/10.1002/cncr.24121 PMID: 19197972
3. Meazza C, Luksch R, Daolio P, Podda M, Luzzati A, Gronchi A, et al. Axial skeletal osteosarcoma: a 25-year monoinstitutional experience in children and adolescents. Med Oncol. 2014;31(4):875. https://doi.org/10.1007/s12032-014-0875-x PMID: 24557586
4. Berger MF, Mardis ER. The emerging clinical relevance of genomics in cancer medicine. Nat Rev Clin Oncol. 2018;15(6):353–65. https://doi.org/10.1038/s41571-018-0002-6 PMID: 29599476
5. Malone ER, Oliva M, Sabatini PJB, Stockley TL, Siu LL. Molecular profiling for precision cancer therapies. Genome Med. 2020;12(1):8. https://doi.org/10.1186/s13073-019-0703-1 PMID: 31937368
6. Rowell JL, McCarthy DO, Alvarez CE. Dog models of naturally occurring cancer. Trends Mol Med. 2011;17(7):380–8. https://doi.org/10.1016/j.molmed.2011.02.004 PMID: 21439907
7. LeBlanc AK, Mazcko CN. Improving human cancer therapy through the evaluation of pet dogs. Nat Rev Cancer. 2020;20(12):727–42. https://doi.org/10.1038/s41568-020-0297-3 PMID: 32934365
8. Farcas N, Arzi B, Verstraete FJM. Oral and maxillofacial osteosarcoma in dogs: a review. Vet Comp Oncol. 2014;12(3):169–80. https://doi.org/10.1111/j.1476-5829.2012.00352.x PMID: 22935032
9. Gardner HL, Sivaprakasam K, Briones N, Zismann V, Perdigones N, Drenner K, et al. Canine osteosarcoma genome sequencing identifies recurrent mutations in DMD and the histone methyltransferase gene SETD2. Commun Biol. 2019;2:266. https://doi.org/10.1038/s42003-019-0487-2 PMID: 31341965

10. Heyman SJ, Diefenderfer DL, Goldschmidt MH, Newton CD. Canine axial skeletal osteosarcoma. A retrospective study of 116 cases (1986 to 1989). Vet Surg. 1992;21(4):304–10. https://doi.org/10.1111/j.1532-950x.1992.tb00069.x PMID: 1455640
11. Ottaviani G, Jaffe N. The epidemiology of osteosarcoma. Cancer Treat Res. 2009;152:3–13. https://doi.org/10.1007/978-1-4419-0284-9_1 PMID: 20213383
12. Tate JG, Bamford S, Jubb HC, Sondka Z, Beare DM, Bindal N. COSMIC: the catalogue of somatic mutations in cancer. Nucleic Acids Res. 2019;47:D941–7.
13. Chen X, Bahrami A, Pappo A, Easton J, Dalton J, Hedlund E, et al. Recurrent somatic structural variations contribute to tumorigenesis in pediatric osteosarcoma. Cell Rep. 2014;7(1):104–12. https://doi.org/10.1016/j.celrep.2014.03.003 PMID: 24703847
14. Chiappetta C, Mancini M, Lessi F, Aretini P, De Gregorio V, Puggioni C, et al. Whole-exome analysis in osteosarcoma to identify a personalized therapy. Oncotarget. 2017;8(46):80416–28. https://doi.org/10.18632/oncotarget.19010 PMID: 29113313
15. Mazcko C, Thomas R. The Establishment of the Pfizer-Canine comparative oncology and genomics consortium biospecimen repository. Vet Sci. 2015;2(3):127–30. https://doi.org/10.3390/vetsci2030127 PMID: 29061936
16. Adalsteinsson VA, Ha G, Freeman SS, Choudhury AD, Stover DG, Parsons HA, et al. Scalable whole-exome sequencing of cell-free DNA reveals high concordance with metastatic tumors. Nat Commun. 2017;8(1):1324. https://doi.org/10.1038/s41467-017-00965-y PMID: 29109393
17. Wang C, Wallerman O, Arendt M-L, Sundström E, Karlsson Å, Nordin J, et al. A novel canine reference genome resolves genomic architecture and uncovers transcript complexity. Commun Biol. 2021;4(1):185. https://doi.org/10.1038/s42003-021-01698-x PMID: 33568770
18. Meadows JRS, Kidd JM, Wang G-D, Parker HG, Schall PZ, Bianchi M, et al. Genome sequencing of 2000 canids by the Dog10K consortium advances the understanding of demography, genome function and architecture. Genome Biol. 2023;24(1):187. https://doi.org/10.1186/s13059-023-03023-7 PMID: 37582787
19. Canis lupus familiaris genome assembly ROS_Cfam_1.0. In: NCBI [Internet]. [cited 12 Jun 2024]. Available from: https://www.ncbi.nlm.nih.gov/datasets/genome/GCF_014441545.1/
20. McKenna A, Hanna M, Banks E, Sivachenko A, Cibulskis K, Kernytsky A, et al. The genome analysis Toolkit: a MapReduce framework for analyzing next-generation DNA sequencing data. Genome Res. 2010;20(9):1297–303. https://doi.org/10.1101/gr.107524.110 PMID: 20644199
21. DePristo MA, Banks E, Poplin R, Garimella KV, Maguire JR, Hartl C, et al. A framework for variation discovery and genotyping using next-generation DNA sequencing data. Nat Genet. 2011;43(5):491–8. https://doi.org/10.1038/ng.806 PMID: 21478889
22. Li H, Durbin R. Fast and accurate short read alignment with Burrows–Wheeler transform. Bioinformatics. 2009;25:1754–60.
23. Kidd J. dogmap: pipeline for dog WGS alignment. Github. Available from: https://github.com/jmkidd/dogmap
24. Benjamin D, Sato T, Cibulskis K, Getz G, Stewart C, Lichtenstein L. Calling Somatic SNVs and Indels with Mutect2. Bioinformatics. 2019. Available from: http://biorxiv.org/lookup/doi/10.1101/861054
25. Kim S, Scheffler K, Halpern AL, Bekritsky MA, Noh E, Källberg M, et al. Strelka2: fast and accurate calling of germline and somatic variants. Nat Methods. 2018;15(8):591–4. https://doi.org/10.1038/s41592-018-0051-x PMID: 30013048
26. Koboldt DC, Zhang Q, Larson DE, Shen D, McLellan MD, Lin L, et al. VarScan 2: Somatic mutation and copy number alteration discovery in cancer by exome sequencing. Genome Res. 2012;22:568–76.
27. Danecek P, Bonfield JK, Liddle J, Marshall J, Ohan V, Pollard MO, et al. Twelve years of SAMtools and BCFtools. Gigascience. 2021;10(2):giab008. https://doi.org/10.1093/gigascience/giab008 PMID: 33590861
28. Gel B, Serra E. KaryoploteR: an R/Bioconductor package to plot customizable genomes displaying arbitrary data. Bioinformatics. 2017;33:3088–90.
29. Jay JJ, Brouwer C. Lollipops in the clinic: information dense mutation plots for precision medicine. PLoS One. 2016;11(8):e0160519. https://doi.org/10.1371/journal.pone.0160519 PMID: 27490490
30. Chen X, Schulz-Trieglaff O, Shaw R, Barnes B, Schlesinger F, Källberg M, et al. Manta: rapid detection of structural variants and indels for germline and cancer sequencing applications. Bioinformatics. 2016;32(8):1220–2. https://doi.org/10.1093/bioinformatics/btv710 PMID: 26647377
31. Sondka Z, Bamford S, Cole CG, Ward SA, Dunham I, Forbes SA. The COSMIC Cancer Gene Census: describing genetic dysfunction across all human cancers. Nat Rev Cancer. 2018;18: 696–705.
32. Sondka Z, Dhir NB, Carvalho-Silva D, Jupe S, Madhumita, McLaren K, et al. COSMIC: a curated database of somatic variants and clinical data for cancer. Nucleic Acids Res. 2024;52: D1210–D1217.
33. Quinlan AR, Hall IM. BEDTools: a flexible suite of utilities for comparing genomic features. Bioinformatics. 2010;26(6):841–2. https://doi.org/10.1093/bioinformatics/btq033 PMID: 20110278
34. Bergstrom EN, Huang MN, Mahto U, Barnes M, Stratton MR, Rozen SG, et al. SigProfilerMatrixGenerator: a tool for visualizing and exploring patterns of small mutational events. BMC Genomics. 2019;20(1):685. https://doi.org/10.1186/s12864-019-6041-2 PMID: 31470794
35. Zhao H, Sun Z, Wang J, Huang H, Kocher J-P, Wang L. CrossMap: a versatile tool for coordinate conversion between genome assemblies. Bioinformatics. 2014;30(7):1006–7. https://doi.org/10.1093/bioinformatics/btt730 PMID: 24351709
36. Gori K, Baez-Ortega A. sigfit: flexible Bayesian inference of mutational signatures. 2020. https://doi.org/10.1101/372896
37. Szklarczyk D, Kirsch R, Koutrouli M, Nastou K, Mehryary F, Hachilif R, et al. The STRING database in 2023: protein-protein association networks and functional enrichment analyses for any sequenced genome of interest. Nucleic Acids Res. 2023;51(D1):D638–46. https://doi.org/10.1093/nar/gkac1000 PMID: 36370105

38. Shannon P, Markiel A, Ozier O, Baliga NS, Wang JT, Ramage D, et al. Cytoscape: a software environment for integrated models of biomolecular interaction networks. Genome Res. 2003;13(11):2498–504. https://doi.org/10.1101/gr.1239303 PMID: 14597658
39. Subramanian A, Tamayo P, Mootha VK, Mukherjee S, Ebert BL, Gillette MA, et al. Gene set enrichment analysis: a knowledge-based approach for interpreting genome-wide expression profiles. Proc Natl Acad Sci U S A. 2005;102(43):15545–50. https://doi.org/10.1073/pnas.0506580102 PMID: 16199517
40. Liberzon A, Subramanian A, Pinchback R, Thorvaldsdóttir H, Tamayo P, Mesirov JP. Molecular signatures database (MSigDB) 3.0. Bioinformatics. 2011;27:1739–40.
41. Milacic M, Beavers D, Conley P, Gong C, Gillespie M, Griss J, et al. The reactome pathway knowledgebase 2024. Nucleic Acids Res. 2024;52:D672–8.
42. Kanehisa M, Goto S. KEGG: kyoto encyclopedia of genes and genomes. Nucleic Acids Res. 2000;28(1):27–30. https://doi.org/10.1093/nar/28.1.27 PMID: 10592173
43. Ashburner M, Ball CA, Blake JA, Botstein D, Butler H, Cherry JM, et al. Gene ontology: tool for the unification of biology. The Gene Ontology Consortium. Nat Genet. 2000;25(1):25–9. https://doi.org/10.1038/75556 PMID: 10802651
44. Gene Ontology Consortium, Aleksander SA, Balhoff J, Carbon S, Cherry JM, Drabkin HJ, et al. The Gene Ontology knowledgebase in 2023. Genetics. 2023;224(1):iyad031. https://doi.org/10.1093/genetics/iyad031 PMID: 36866529
45. Uhlen M, Oksvold P, Fagerberg L, Lundberg E, Jonasson K, Forsberg M, et al. Towards a knowledge-based Human Protein Atlas. Nat Biotechnol. 2010;28(12):1248–50. https://doi.org/10.1038/nbt1210-1248 PMID: 21139605
46. Uhlén M, Fagerberg L, Hallström BM, Lindskog C, Oksvold P, Mardinoglu A, et al. Proteomics. Tissue-based map of the human proteome. Science. 2015;347(6220):1260419. https://doi.org/10.1126/science.1260419 PMID: 25613900
47. Coyle VJ, Rassnick KM, Borst LB, Rodriguez COJ, Northrup NC, Fan TM. Biological behaviour of canine mandibular osteosarcoma. A retrospective study of 50 cases (1999-2007). Vet Comp Oncol. 2015;13:89–97.
48. Straw RC, Powers BE, Klausner J, Henderson RA, Morrison WB, McCaw DL. Canine mandibular osteosarcoma: 51 cases (1980-1992). J Am Anim Hosp Assoc. 1996;32:257–62.
49. Sakthikumar S, Elvers I, Kim J, Arendt ML, Thomas R. SETD2 Is Recurrently Mutated in Whole-Exome Sequenced Canine OsteosarcomaMutational Landscape in Canine Osteosarcoma. Cancer Res. 2018. Available from: https://aacrjournals.org/cancerres/article-abstract/78/13/3421/628258
50. Das S, Idate R, Regan DP, Fowles JS, Lana SE, Thamm DH, et al. Immune pathways and TP53 missense mutations are associated with longer survival in canine osteosarcoma. Commun Biol. 2021;4(1):1178. https://doi.org/10.1038/s42003-021-02683-0 PMID: 34635775
51. Buddingh EP, Kuijjer ML, Duim RAJ, Bürger H, Agelopoulos K, Myklebost O, et al. Tumor-infiltrating macrophages are associated with metastasis suppression in high-grade osteosarcoma: a rationale for treatment with macrophage activating agents. Clin Cancer Res. 2011;17(8):2110–9. https://doi.org/10.1158/1078-0432.CCR-10-2047 PMID: 21372215
52. Wang F, Zhao Q, Liu W, Kong D. CENPE, PRC1, TTK, and PLK4 may play crucial roles in the osteosarcoma progression. Technol Cancer Res Treat. 2020;19.
53. Megquier K, Turner-Maier J, Morrill K, Li X, Johnson J, Karlsson EK, et al. The genomic landscape of canine osteosarcoma cell lines reveals conserved structural complexity and pathway alterations. PLoS One. 2022;17(9):e0274383. https://doi.org/10.1371/journal.pone.0274383 PMID: 36099278
54. Meng F, Zhou X, Zhao Z, Pei L, Xia W. Discovery of core genes and intercellular communication role in osteosarcoma. J Appl Genet. 2025;66(2):323–32. https://doi.org/10.1007/s13353-024-00872-1 PMID: 38814547
55. Mayers J. Investigation of the effects of alterations in the glutamate receptor, GRIK2 on osteosarcoma tumourigenesis. Doctor of Philosophy, University of Toronto. 2019. Available from: https://tspace.library.utoronto.ca/bitstream/1807/95915/1/Mayers_Justin_201906_PhD_thesis.pdf
56. Mayakonda A, Lin D-C, Assenov Y, Plass C, Koeffler HP. Maftools: efficient and comprehensive analysis of somatic variants in cancer. Genome Res. 2018;28(11):1747–56. https://doi.org/10.1101/gr.239244.118 PMID: 30341162
57. Shao YW, Wood GA, Lu J, Tang Q-L, Liu J, Molyneux S, et al. Cross-species genomics identifies DLG2 as a tumor suppressor in osteosarcoma. Oncogene. 2019;38(2):291–8. https://doi.org/10.1038/s41388-018-0444-4 PMID: 30093633
58. Kaspar P, Dvoráková M, Králová J, Pajer P, Kozmik Z, Dvorák M. Myb-interacting protein, ATBF1, represses transcriptional activity of Myb oncoprotein. J Biol Chem. 1999;274:14422–8.
59. Chu S, Skidmore ZL, Kunisaki J, Walker JR, Griffith M, Griffith OL, et al. Unraveling the chaotic genomic landscape of primary and metastatic canine appendicular osteosarcoma with current sequencing technologies and bioinformatic approaches. PLoS One. 2021;16(2):e0246443. https://doi.org/10.1371/journal.pone.0246443 PMID: 33556121
60. Schaub FX, Dhankani V, Berger AC, Trivedi M, Richardson AB, Shaw R, et al. Pan-cancer alterations of the MYC oncogene and its proximal network across the cancer genome atlas. Cell Syst. 2018;6(3):282-300.e2. https://doi.org/10.1016/j.cels.2018.03.003 PMID: 29596783
61. Shorthouse D, Zhuang L, Rahrmann EP, Kosmidou C, Wickham Rahrmann K, Hall M, et al. KCNQ potassium channels modulate Wnt activity in gastro-oesophageal adenocarcinomas. Life Sci Alliance. 2023;6(12):e202302124. https://doi.org/10.26508/lsa.202302124 PMID: 37748809
62. Bottos A, Destro E, Rissone A, Graziano S, Cordara G, Assenzio B, et al. The synaptic proteins neurexins and neuroligins are widely expressed in the vascular system and contribute to its functions. Proc Natl Acad Sci U S A. 2009;106(49):20782–7. https://doi.org/10.1073/pnas.0809510106 PMID: 19926856

63. Bottos A, Rissone A, Bussolino F, Arese M. Neurexins and neuroligins: synapses look out of the nervous system. Cell Mol Life Sci. 2011;68:2655–66.
64. Graziano S, Marchiò S, Bussolino F, Arese M. A peptide from the extracellular region of the synaptic protein α Neurexin stimulates angiogenesis and the vascular specific tyrosine kinase Tie2. Biochem Biophys Res Commun. 2013;432(4):574–9. https://doi.org/10.1016/j.bbrc.2013.02.045 PMID: 23485462
65. Pergolizzi M, Bizzozero L, Maione F, Maldi E, Isella C, Macagno M, et al. The neuronal protein Neuroligin 1 promotes colorectal cancer progression by modulating the APC/β-catenin pathway. J Exp Clin Cancer Res. 2022;41(1):266. https://doi.org/10.1186/s13046-022-02465-4 PMID: 36056393
66. Yotsumoto T, Maemura K, Watanabe K, Amano Y, Matsumoto Y, Zokumasu K, et al. NRXN1 as a novel potential target of antibody-drug conjugates for small cell lung cancer. Oncotarget. 2020;11(39):3590–600. https://doi.org/10.18632/oncotarget.27718 PMID: 33062195
67. Roundhill EA, Chicon-Bosch M, Jeys L, Parry M, Rankin KS, Droop A, et al. RNA sequencing and functional studies of patient-derived cells reveal that neurexin-1 and regulators of this pathway are associated with poor outcomes in Ewing sarcoma. Cell Oncol (Dordr). 2021;44(5):1065–85. https://doi.org/10.1007/s13402-021-00619-8 PMID: 34403115
68. Xie X, Li Y, Su S, Li X, Xu X, Gao Y, et al. Neuroligins facilitate the development of bone cancer pain via regulating synaptic transmission: an experimental study. Braz J Anesthesiol. 2024;74(4):744422. https://doi.org/10.1016/j.bjane.2023.02.001 PMID: 36841430